JOURNAL OF PROPULSION AND POWER
Vol. 16, No. 2, March–April 2000

Detailed Chemical-Kinetic Model for Aviation Fuels

R. P. Lindstedt*
Imperial College of Science, Technology, and Medicine, London, England SW7 2BX, United Kingdom
and
L. Q. Maurice†
U.S. Air Force Research Laboratory, Wright–Patterson Air Force Base, Ohio 45433-7103

The introduction of detailed chemical reaction mechanisms for aviation fuels into complex multidimensional fluid dynamics problems is not practical at the present time. Simplified reaction mechanisms that have been thoroughly evaluated must be developed to address specific issues arising in realistic combustor configurations. The latter should be firmly based on detailed mechanisms carefully evaluated against a wide range of experimental data. A detailed kinetic mechanism for hydrocarbon combustion is formulated to address the gas-phase chemistry of endothermic and conventional aviation fuels. Reaction paths are analysed for *n*-decane and kerosene premixed flames, and the ability of the mechanism to predict various premixed flame features is assessed by comparison with experimental species profiles. Finally, the level of success achieved by the present kinetic model in the context of practical problems is discussed.

Introduction

As a step toward enabling the detailed modeling of the gas-phase chemistry of aviation fuels, a detailed chemical–kinetic mechanism applicable to hydrocarbons has been developed and evaluated systematically in previous work.[1–6] The resulting mechanism appears to constitute an excellent starting point for the development of kinetic models for aviation fuels, as it contains basic alkane, monosubstituted aromatic (MSA), and polycyclic aromatic hydrocarbons (PAH) chemistry. The next logical step is clearly to evaluate the capability of the model to predict the gas-phase chemistry of practical aviation fuels. Consequently, the combustion chemistry of prototype endothermic (fuels which feature an additional heat sink over conventional hydrocarbon fuels by undergoing sensible heating and deliberate bulk fuel reactions supported by the energy extracted from aerodynamically heated air) and conventional aviation fuels is addressed in this paper.

The majority of research efforts involving endothermic fuels have been directed toward the development of catalysts and heat exchanger/reactor systems that enable the application of the technology at reasonable temperatures and pressures in flight-weight hardware.[7,8] The fundamental combustion behavior of these fuels, however, has received comparatively little study.[9] Experiments aimed at studying the combustion characteristics of endothermic fuels have been limited to measurements of flame speeds and autoignition temperatures in simplified geometries.[10,11] Detailed chemical kinetic modeling efforts have not been undertaken prior to the present work.

The endothermic cracking of normal paraffins has been investigated experimentally by Sobel and Spadaccini.[8] The product efflux consisted primarily of low-molecular-weight alkenes and alkanes (ethylene, propene, propane, ethane, and methane) and hydrogen. An actual chemical endotherm of about 1100 kJ/kg was measured. The ability of the present hierarchically constructed mechanism to capture the combustion kinetics of the products of the endothermic conversion process has been previously shown.[1–5] Thus, the present extension of the mechanism to higher-order hydrocarbons is aimed at producing a predictive tool applicable to the parent endothermic fuel as well as to the products of endothermic reactions.

Received 12 September 1997; revision received 5 March 1999; accepted for publication 16 March 1999. This paper is declared a work of the U.S. Government and is not subject to copyright protection in the United States.

*Reader, Mechanical Engineering Department, Exhibition Road. Member AIAA.

†Senior Research Scientist, Propulsion Directorate, Fuels Branch, 1790 Loop Rd. N. Associate Fellow AIAA.

Kinetic studies of kerosene aviation fuels have generally been considered prohibitive. As a first approximation, Guéret et al.[12] modeled kerosene oxidation via quasiglobal models for *n*-decane, *n*-propylcyclohexane, trimethyl benzene, xylene, toluene, and benzene and recognized the need for further refinement of the aromatic models. Dagaut et al.[13] modeled kerosene combustion in jet-stirred reactors using *n*-decane as a reference hydrocarbon while neglecting the aromatic components. Ranzi et al.[14] proposed a comprehensive reaction mechanism for higher-order hydrocarbon fuels that only considers benzene in a semi-empirical manner. Vovelle et al.[15] studied reduced-pressure kerosene flames and modeled the aromatic component with a simplified toluene mechanism. Discrepancies between computations and experimental observations were predominantly attributed to uncertainties in the aromatic model. The cited studies recognized the need to include an aromatic submechanism, preferably considering MSA molecules, in detailed kerosene kinetic modeling. However, aromatic detailed kinetic submechanisms evaluated over a broad range of experimental conditions have not been previously available. The work of Lindstedt and Maurice[6] and Maurice[16] on MSA and PAH oxidation has provided an aromatic submechanism suitable for extension to the modeling of aviation fuels.

n-Decane Combustion

Mechanistic Considerations

A potentially practical endothermic fuel such as Norpar 12® (a blend of normal paraffins with average carbon number 12) would have to be blended with lower-order hydrocarbons to meet volatility and freeze point specifications for aviation fuels.[8] Thus, the final blend will conceivably have an average carbon number closer to C_{10}. Consequently, it is reasonable to study the combustion kinetics of *n*-decane as a prototype for endothermic fuels.

It is well established that large-molecular-weight saturated hydrocarbons such as *n*-decane are primarily consumed through pyrolysis and H abstraction in combustion environments.[17] However, experimentally determined kinetic rate data for *n*-decane pyrolysis and H abstraction reactions are virtually nonexistent. Lindstedt and Maurice[3] found that the rates for *n*-heptane pyrolysis proposed by Chakir et al.[18] on the basis of intermediate temperature-stirred reactors were problematic at flame temperatures. A rate for *n*-heptane pyrolysis fitted on the basis of experimental data has been shown to reconcile experimental observations in both combustion regimes.[3] Thus, a rate expression for the total *n*-decane pyrolysis rate has been fitted to experimental data[19,20] in the present work. The products of *n*-decane pyrolysis were assigned based on analogy with

observations for *n*-heptane pyrolysis with branching ratios subsequently adjusted as a result of the evaluation procedure.

The rates of the *n*-decane H abstraction reactions adopted in the present work were estimated using additivity techniques as proposed by Warnatz.[17] The accuracy of the latter estimates has been postulated to be within a factor of two by Miller et al.[21] The resulting *n*-decyl radicals are assumed to be consumed via pyrolysis reactions yielding alkene and smaller alkyl radical molecules, as suggested by Warnatz.[22] Isomerization reactions for the *n*-decyl radicals are also considered, and rates for the latter are estimated based on analogy with *n*-heptane. Overall, the extension of the mechanism to consider *n*-decane combustion is accomplished by the addition of 64 elementary reactions and 8 species. The final comprehensive detailed reaction mechanism thus comprises 193 chemical species and 1085 elementary reactions. The rate constants for the *n*-decane submechanism are shown in Table 1 (see Refs. 19, 20, 23, and 24). The

Table 1 Elementary reactions for *n*-decane submechanism

Reaction[a]			*A*	*n*	*E*	Reference
$C_{10}H_{22}$	⇔	1-C_7H_{15} + n-C_3H_7	7.850*E*+14	0.00	283.90	Fitted[19,20]
$C_{10}H_{22}$	⇔	1-C_5H_{11} + 1-C_5H_{11}	7.850*E*+14	0.00	283.90	Fitted[19,20]
$C_{10}H_{22}$	⇔	1-C_6H_{13} + p-C_4H_9	1.047*E*+15	0.00	283.90	Fitted[19,20]
$C_{10}H_{22}$	⇔	1-$C_{10}H_{21}$ + H	8.000*E*+14	0.00	424.00	Estimated
$C_{10}H_{22}$	⇔	2-$C_{10}H_{21}$ + H	8.000*E*+14	0.00	424.00	Estimated
$C_{10}H_{22}$	⇔	3-$C_{10}H_{21}$ + H	8.000*E*+14	0.00	424.00	Estimated
$C_{10}H_{22}$	⇔	4-$C_{10}H_{21}$ + H	8.000*E*+14	0.00	424.00	Estimated
$C_{10}H_{22}$	⇔	5-$C_{10}H_{21}$ + H	8.000*E*+14	0.00	424.00	Estimated
$C_{10}H_{22}$ + H	⇔	1-$C_{10}H_{21}$ + H_2	4.700*E*+04	2.00	32.20	Estimated
$C_{10}H_{22}$ + H	⇔	2-$C_{10}H_{21}$ + H_2	1.500*E*+04	2.00	20.92	Estimated
$C_{10}H_{22}$ + H	⇔	3-$C_{10}H_{21}$ + H_2	1.500*E*+04	2.00	20.92	Estimated
$C_{10}H_{22}$ + H	⇔	4-$C_{10}H_{21}$ + H_2	1.500*E*+04	2.00	20.92	Estimated
$C_{10}H_{22}$ + H	⇔	5-$C_{10}H_{21}$ + H_2	1.500*E*+04	2.00	20.92	Estimated
$C_{10}H_{22}$ + OH	⇔	1-$C_{10}H_{21}$ + H_2O	4.400*E*+06	0.97	6.65	Estimated
$C_{10}H_{22}$ + OH	⇔	2-$C_{10}H_{21}$ + H_2O	1.960*E*+04	1.61	0.00	Estimated
$C_{10}H_{22}$ + OH	⇔	3-$C_{10}H_{21}$ + H_2O	1.960*E*+04	1.61	0.00	Estimated
$C_{10}H_{22}$ + OH	⇔	4-$C_{10}H_{21}$ + H_2O	1.960*E*+04	1.61	0.00	Estimated
$C_{10}H_{22}$ + OH	⇔	5-$C_{10}H_{21}$ + H_2O	1.960*E*+04	1.61	0.00	Estimated
$C_{10}H_{22}$ + O	⇔	1-$C_{10}H_{21}$ + OH	1.920*E*+03	2.40	6.65	Estimated
$C_{10}H_{22}$ + O	⇔	2-$C_{10}H_{21}$ + OH	5.330*E*+02	2.50	20.92	Estimated
$C_{10}H_{22}$ + O	⇔	3-$C_{10}H_{21}$ + OH	5.330*E*+02	2.50	20.92	Estimated
$C_{10}H_{22}$ + O	⇔	4-$C_{10}H_{21}$ + OH	5.330*E*+02	2.50	20.92	Estimated
$C_{10}H_{22}$ + O	⇔	5-$C_{10}H_{21}$ + OH	5.330*E*+02	2.50	20.92	Estimated
$C_{10}H_{22}$ + CH_3	⇔	1-$C_{10}H_{21}$ + CH_4	2.500*E*+09	0.00	48.53	Estimated
$C_{10}H_{22}$ + CH_3	⇔	2-$C_{10}H_{21}$ + CH_4	1.330*E*+09	0.00	39.75	Estimated
$C_{10}H_{22}$ + CH_3	⇔	3-$C_{10}H_{21}$ + CH_4	1.330*E*+09	0.00	39.75	Estimated
$C_{10}H_{22}$ + CH_3	⇔	4-$C_{10}H_{21}$ + CH_4	1.330*E*+09	0.00	39.75	Estimated
$C_{10}H_{22}$ + CH_3	⇔	5-$C_{10}H_{21}$ + CH_4	1.330*E*+09	0.00	39.75	Estimated
$C_{10}H_{22}$ + HO_2	⇔	1-$C_{10}H_{21}$ + H_2O_2	9.330*E*+09	0.00	81.17	Estimated
$C_{10}H_{22}$ + HO_2	⇔	2-$C_{10}H_{21}$ + H_2O_2	5.670*E*+09	0.00	71.13	Estimated
$C_{10}H_{22}$ + HO_2	⇔	3-$C_{10}H_{21}$ + H_2O_2	5.670*E*+09	0.00	71.13	Estimated
$C_{10}H_{22}$ + HO_2	⇔	4-$C_{10}H_{21}$ + H_2O_2	5.670*E*+09	0.00	71.13	Estimated
$C_{10}H_{22}$ + HO_2	⇔	5-$C_{10}H_{21}$ + H_2O_2	5.670*E*+09	0.00	71.13	Estimated
$C_{10}H_{22}$ + O_2	⇔	1-$C_{10}H_{21}$ + HO_2	2.090*E*+10	0.00	218.12	Estimated
$C_{10}H_{22}$ + O_2	⇔	2-$C_{10}H_{21}$ + HO_2	3.300*E*+10	0.00	204.00	Estimated
$C_{10}H_{22}$ + O_2	⇔	3-$C_{10}H_{21}$ + HO_2	3.300*E*+10	0.00	204.00	Estimated
$C_{10}H_{22}$ + O_2	⇔	4-$C_{10}H_{21}$ + HO_2	3.300*E*+10	0.00	204.00	Estimated
$C_{10}H_{22}$ + O_2	⇔	5-$C_{10}H_{21}$ + HO_2	3.300*E*+10	0.00	204.00	Estimated
1-$C_{10}H_{21}$	⇔	C_8H_{17} + C_2H_4	2.100*E*+13	0.00	121.00	Estimated
2-$C_{10}H_{21}$	⇔	1-C_7H_{15} + C_3H_6	2.100*E*+13	0.00	110.00	Estimated
3-$C_{10}H_{21}$	⇔	1-C_6H_{13} + 1-C_4H_8	2.100*E*+13	0.00	110.00	Estimated
4-$C_{10}H_{21}$	⇔	1-C_5H_{11} + 1-C_5H_{10}	2.100*E*+13	0.00	107.00	Estimated
4-$C_{10}H_{21}$	⇔	C_8H_{16} + C_2H_5	1.000*E*+13	0.00	121.00	Estimated
5-$C_{10}H_{21}$	⇔	1-C_6H_{12} + p-C_4H_9	4.200*E*+13	0.00	108.00	Estimated
5-$C_{10}H_{21}$	⇔	1-C_7H_{14} + n-C_3H_7	2.100*E*+13	0.00	121.00	Estimated
1-$C_{10}H_{21}$	⇔	4-$C_{10}H_{21}$	2.000*E*+11	0.00	84.00	Estimated
1-$C_{10}H_{21}$	⇔	5-$C_{10}H_{21}$	2.000*E*+11	0.00	84.00	Estimated
2-$C_{10}H_{21}$	⇔	4-$C_{10}H_{21}$	2.000*E*+11	0.00	84.00	Estimated
2-$C_{10}H_{21}$	⇔	5-$C_{10}H_{21}$	2.000*E*+11	0.00	84.00	Estimated
3-$C_{10}H_{21}$	⇔	4-$C_{10}H_{21}$	2.000*E*+11	0.00	84.00	Estimated
3-$C_{10}H_{21}$	⇔	5-$C_{10}H_{21}$	2.000*E*+11	0.00	84.00	Estimated
C_8H_{17}	⇔	C_8H_{16} + H	2.000*E*+13	0.00	158.99	23
C_8H_{17}	⇔	1-C_7H_{14} + CH_3	7.940E+13	0.00	138.07	24
C_8H_{17}	⇔	1-C_6H_{13} + C_2H_4	2.510*E*+13	0.00	120.50	24
C_8H_{17}	⇔	1-C_5H_{11} + C_3H_6	1.580*E*+13	0.00	118.41	24
C_8H_{17}	⇔	1-C_5H_{10} + n-C_3H_7	5.010*E*+12	0.00	121.75	24
C_8H_{17}	⇔	p-C_4H_9 + 1-C_4H_8	5.010*E*+12	0.00	121.75	24
C_8H_{17} + O_2	⇔	C_8H_{16} + HO_2	4.000*E*+09	0.00	8.37	23
C_8H_{16}	⇔	1-C_5H_{11} + a-C_3H_5	2.000E+15	0.00	297.48	24
C_8H_{16}	⇔	p-C_4H_9 + C_4H_7	1.000*E*+16	0.00	342.25	24
C_8H_{16} + O	⇔	1-C_7H_{15} + CHO	1.000*E*+08	0.00	0.00	24
C_8H_{16} + O	⇔	1-C_6H_{13} + C_2H_3O	1.000*E*+08	0.00	0.00	24
C_8H_{16} + OH	⇔	1-C_7H_{15} + CH_2O	1.000*E*+08	0.00	0.00	24
C_8H_{16} + OH	⇔	1-C_6H_{13} + C_2H_4O	1.000*E*+08	0.00	0.00	24

[a]Reaction rates are expressed in the form: $k = AT^n \exp(-E_a/RT)$ where A is the frequency factor, $(\text{kmol/m}^3)^{1-m}/\text{s}$, in which m is the order of the reaction; n is the temperature dependence exponent; E_a is the activation energy, kJ/kmole; R is the ideal gas constant, 8.314 kJ/K/kmole; and T is temperature, K.

rate constants for the remaining elementary reactions and pertinent thermodynamic and transport data are as reported elsewhere.[3,6,16] The development of the mechanism has placed particular emphasis on the chemical complexities of flames at temperatures >1000 K at atmospheric pressures.

Comparison with Experiments

It is generally recognized that premixed laminar flames constitute an attractive medium in which to study combustion chemistry.[21,22] Such flames retain important transport features, which are not discernible in spatially homogeneous reactors. Thus, the *n*-decane combustion submechanism has been evaluated by comparison to experimental profiles for major, stable intermediate and radical species in two rich, *n*-decane laminar premixed flames stabilized on flat flame burners. Computational procedures are as previously reported.[4,16] Laminar premixed flames are computed using a numerical code developed by Jones and Lindstedt.[25,26] Freely propagating flames are assumed to be bounded by two propagating points at the unburned and burned boundaries. The species concentrations and enthalpy of the mixture are specified at the unburned boundary, and the species and enthalpy gradients at the burned boundary are set equal to zero. Subsequently, the solution is allowed to march in time until the reaction integrals for all species are equal. The experimental temperature profiles and mass flow rates are imposed on the computations of burner stabilized flames, and only the species concentrations are determined. The latter approach lessens uncertainties due to burner heat losses. Douté et al.[27] measured the structure of a rich ($\phi = 1.7$), atmospheric pressure, 3.2% *n*-decane/28.6% O_2/68.2% N_2 flame. Temperature profiles were measured using Pt–Pt 10% Rh thermocouples, and the accuracy of the location of the probe tip was estimated at 0.05 mm. Reported uncertainties in temperature measurements were within ±100 K. Gas samples were obtained through quartz microprobes and analyzed via gas chromatography. Delfau et al.[28] measured the structure of a sooting ($\phi = 1.9$), 0.06-bar, 5.1% *n*-decane/41.2% O_2/53.7% Ar flame. Temperature profiles were measured also using Pt–Pt 10% Rh thermocouples. Gas samples were obtained through quartz cones and analysed via molecular beam mass spectroscopy. Concentration profiles for stable and radical species were reported. The temperature profiles for the flame of Delfau et al.[28] are subject to large uncertainties, and the data sets must be viewed with corresponding caution.

Comparisons between experimental and computed *n*-decane decay profiles for the atmospheric pressure flame of Douté et al.[27] are shown in Fig. 1. The sensitivity of the computed profiles to 1) the reported experimental uncertainties in the temperature profile[27] and 2) uncertainty factors of $x/5$ for total *n*-decane fuel consumption rates also are shown. The model captures the fuel decay profile accurately and correctly predicts the disappearance of the fuel within 1 mm. The disappearance of oxygen within 2 mm is also predicted accurately. The fuel decay profile is observed to be more sensitive to decreases in the fuel consumption rates than to similar increases. Furthermore, sensitivity responses to the uncertainties in the fuel decay rates are less significant than observed for uncertainties in the measured temperature profile.

The computed growth profiles for major species exhibit spatial location sensitivities to uncertainties in the experimental temperature profile, but are unaffected by the uncertainties in fuel consumption rates. Predictions of CO and CO_2 are in excellent agreement with experimental observations for the atmospheric pressure flame of Douté et al.[27] (Fig. 2), but underpredicted by about 15% for the 0.06-bar flame of Delfau et al.[28] (Fig. 3). The experimentally observed CO/CO_2 ratios are predicted well for both flames. Molecular hydrogen concentrations are predicted well in the primary zone, but underpredicted by about 30% in the postflame zone for the atmospheric pressure flame. Computed H_2 concentrations are in good agreement with experimental values for the 0.06-bar flame (Fig. 3). Predictions of water concentrations are reasonable and in excellent agreement in the postflame zone for both flames.

Comparisons between experimental and computed H atom and OH radical profiles for the 0.06-bar flame of Delfau et al.[28] are shown in Fig. 4. The experimental profiles exhibit some peculiar characteristics. No notable growth of H atoms is observed in a location

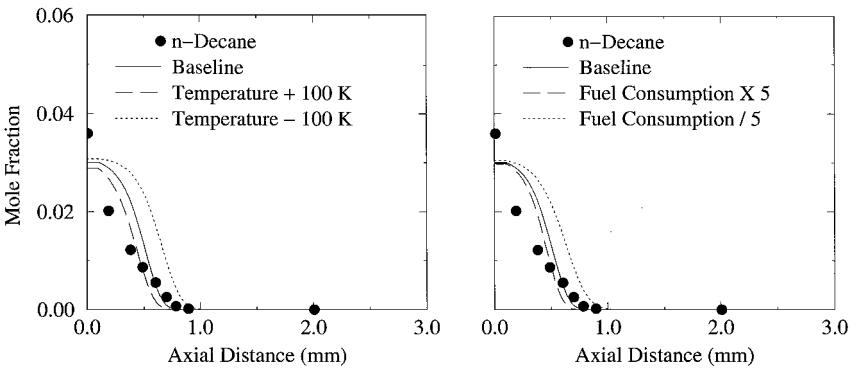

Fig. 1 Sensitivities of *n*-decane decay to uncertainties in the temperature profile and the fuel consumption rates in a rich, atmospheric-pressure *n*-decane/O_2/N_2 laminar premixed flame; symbols indicate experimental data,[27] and lines indicate computations.

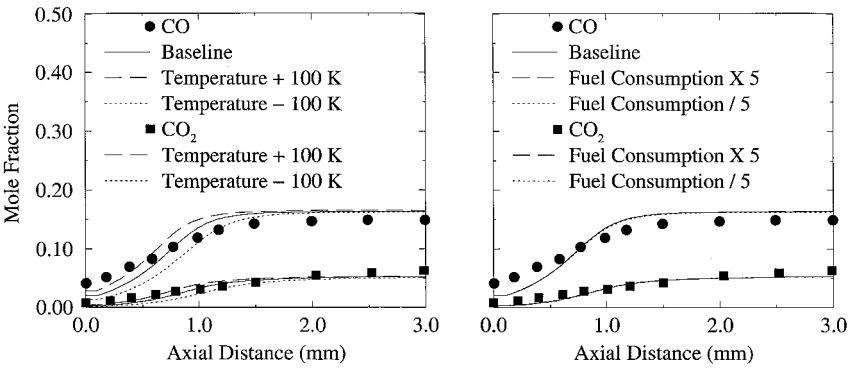

Fig. 2 Sensitivities of CO and CO_2 concentrations to uncertainties in the temperature profile and the fuel consumption rates in a rich, atmospheric-pressure *n*-decane/O_2/N_2 laminar premixed flame; symbols indicate experimental data,[27] and lines indicate computations.

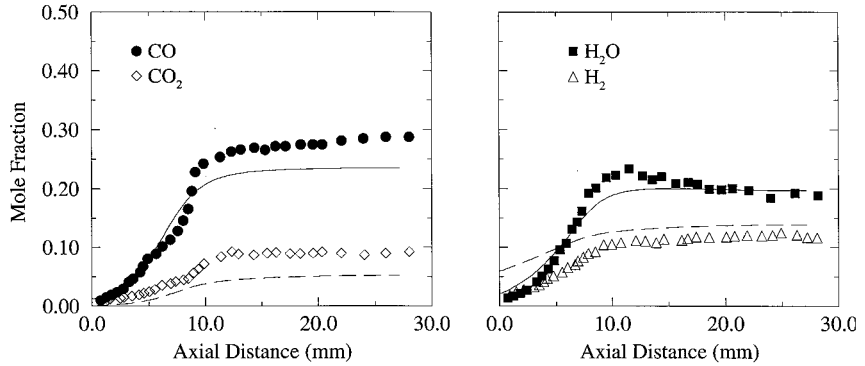

Fig. 3 CO, CO_2, H_2, and H_2O concentrations in a rich, 0.06-bar *n*-decane/O_2/Ar laminar premixed flame, symbols indicate experimental data,[28] and lines indicate computations.

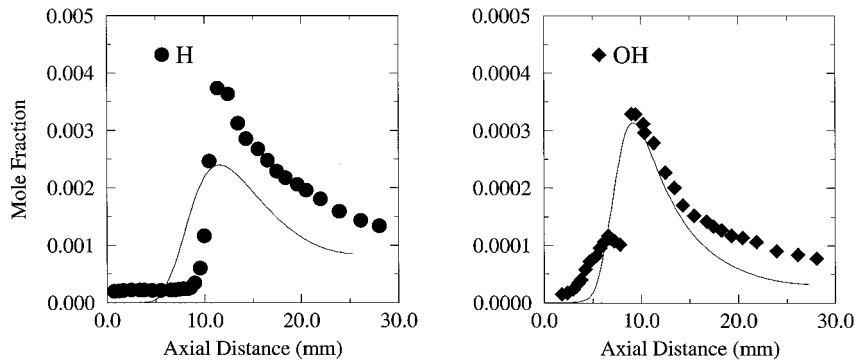

Fig. 4 H and OH concentrations in a rich, 0.06-bar *n*-decane/O_2/Ar laminar premixed flame; symbols indicate experimental data,[28] and lines indicate computations.

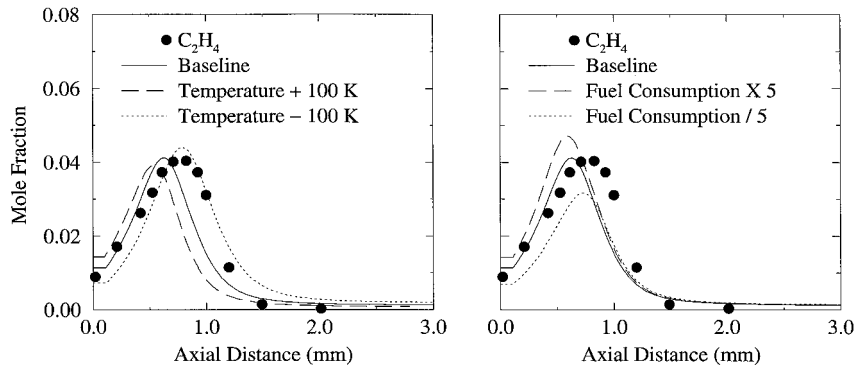

Fig. 5 Sensitivities of C_2H_4 concentrations to uncertainties in the temperature profile and the fuel consumption rates in a rich, atmospheric-pressure *n*-decane/O_2/N_2 laminar premixed flame; symbols indicate experimental data,[27] and lines indicate computations.

in the primary zone where OH radical concentrations are clearly increasing. Clearly, such behavior is unusual given the higher diffusivity of the H atom. In addition, the OH radical profile features an unusual bimodal character. The peak concentration of the H atom is underpredicted by about 70%. The disagreement in the H atom concentrations is attributable to uncertainties in the temperature profile and the species measurements, as well as to mechanistic uncertainties. Increasing the imposed temperature profile by +100 K (within the experimental uncertainty) leads to overprediction of H atom concentrations. Predictions of OH radical concentrations in laminar premixed flames do not exhibit a strong dependence to the experimental temperature profiles, and, the peak concentration is predicted well.

The primary intermediates observed in *n*-decane flames are ethylene, acetylene, methane, propene, and ethane in decreasing order of concentration. The spatial profile and maximum concentration of ethylene (Fig. 5) in the atmospheric-pressure flame of Douté et al.[27] is captured well. The concentration profiles of acetylene, methane, and ethane for the atmospheric-pressure flame of Douté et al.[27] are predicted reasonably well. The magnitude and location of the maximum concentration of acetylene (Fig. 6) are captured within the experimental uncertainties of the temperature profiles. The computed decay of acetylene in the postflame zone is somewhat slower than is observed experimentally.

Comparisons between measurements and computations for allene and propyne in the flame of Douté et al.[27] are shown in Figs. 7 and 8. Peak concentrations of allene are underpredicted by about 40%, whereas propyne peak concentrations are predicted well. Allene is produced primarily via the decomposition of the allyl radical, and the latter is consumed principally through molecular oxygen attack reactions.[29] The reaction rates and product branching ratios for reactions between unsaturated radicals and molecular oxygen are

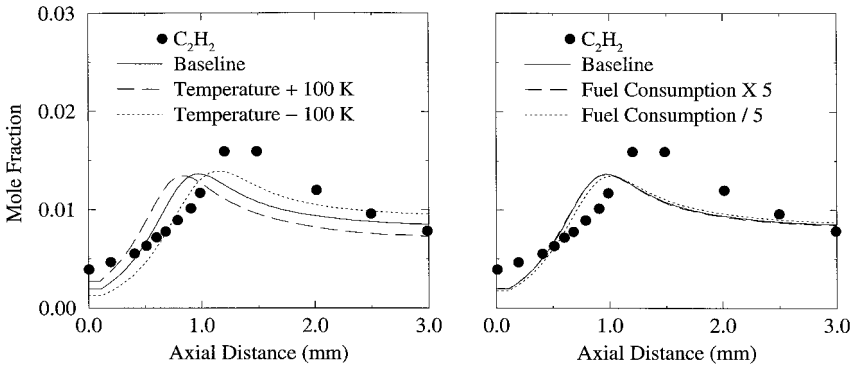

Fig. 6 Sensitivities of C_2H_2 concentrations to uncertainties in the temperature profile and the fuel consumption rates in a rich, atmospheric-pressure *n*-decane/O_2/N_2 laminar premixed flame; symbols indicate experimental data,[27] and lines indicate computations.

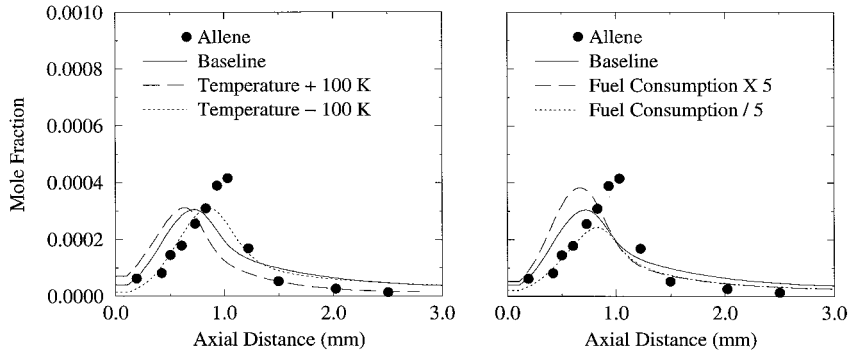

Fig. 7 Sensitivities of allene concentrations to uncertainties in the temperature profile and the fuel consumption rates in a rich, atmospheric-pressure *n*-decane/O_2/N_2 laminar premixed flame; symbols indicate experimental data,[27] and lines indicate computations.

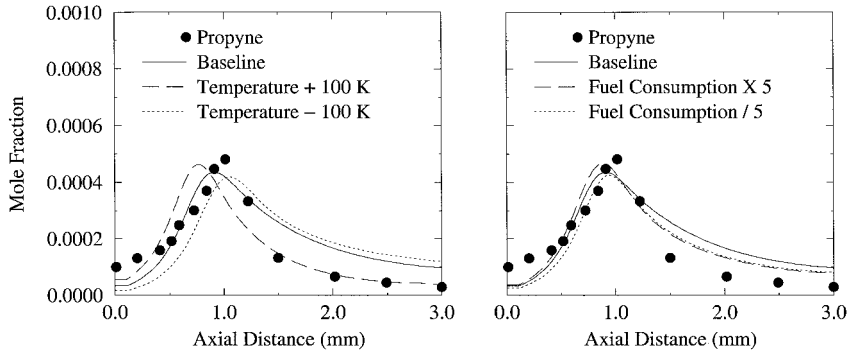

Fig. 8 Sensitivities of propyne concentrations to uncertainties in the temperature profile and the fuel consumption rates in a rich, atmospheric-pressure *n*-decane/O_2/N_2 laminar premixed flame; symbols indicate experimental data,[27] and lines indicate computations.

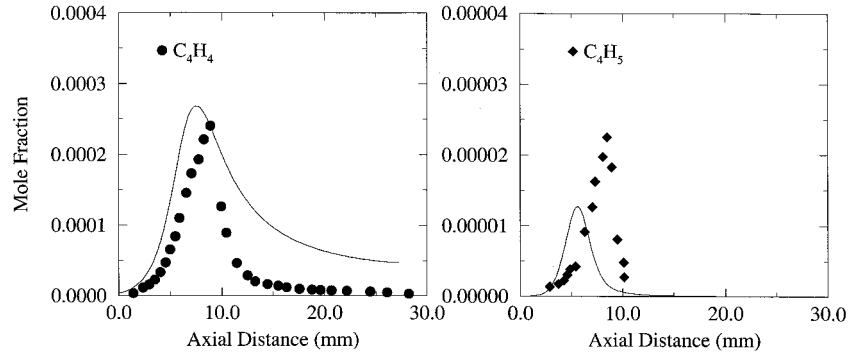

Fig. 9 C_4H_4 and C_4H_5 concentrations in a rich, 0.06-bar *n*-decane/O_2/Ar laminar premixed flame; symbols indicate experimental data,[28] and lines indicate computations.

problematic, and the allyl radical is no exception. The rate of decay of allene in the postflame region is correctly modeled, whereas that of propyne is reasonably predicted within reported experimental uncertainties. The concentration profile for vinyl acetylene in the 0.06-bar flame (Fig. 9) is predicted reasonably well. Finally, the peak concentration of the butadienyl radicals, experimentally observed to be less than 25 ppm, is predicted within a factor of two. The satisfactory predictions of acetylene, propyne, allene, vinyl acetylene, and the butadienyl radicals concentrations are encouraging in the context of the study of benzene formation paths outlined next.

Benzene Formation

The accurate prediction of aromatic destruction/ring formation in practical aliphatic aviation fuels is clearly a topic of interest in soot and pollutant formation studies. The benzene formation steps from noncyclic hydrocarbons considered here are as reported previously.[5,16,29] The primary benzene formation channels for *n*-decane premixed flames are shown in Fig. 10. Benzene is predominantly (60%) formed via propargyl radical recombination through linear C_6H_6 species and fulvene.[2,5] Acetylene addition to the (1, 3)-butadienyl radical and vinyl radical addition to vinylacetylene each contributes about 15% of the total.

Comparisons between measured and computed benzene profiles are shown in Figs. 11 and 12. Clearly, both the shape and peak concentration of the benzene profile in the primary zone of the low-pressure flame are very well predicted. By contrast, the prediction of the peak benzene concentration in the atmospheric pressure flame exhibits an error around 50%, and a spatial offset is noted. The rate of benzene decay in the postflame zone is clearly underpredicted for both flames. The propargyl radical recombination reactions are strongly partially equilibrated, and consequently, the location of the peak concentration of benzene and the rate of decay in the postflame zone display a strong sensitivity to the temperature profile. Increasing the temperature profile imposed on the computations by 100 K leads to acceptable predictions of benzene decay in the postflame zone as is evident in Figs. 11 and 12. The peak benzene concentration also is observed to be sensitive to decreases in the fuel consumption rates, but remains essentially unaffected by similar increases. Not surprisingly, the postflame zone is unaffected by the uncertainties in the fuel consumption rates.

Kerosene Combustion: Mechanistic Considerations

The species concentration profiles measured by Douté et al.[27] for a laminar premixed kerosene (jet A) flame are the most comprehensive data sets for kerosene oxidation reported to date. The complexities associated with the chemical composition of kerosene-type fuels is well recognized,[16] and a detailed computational consideration of all of the fuel components of kerosene would be prohibitive. Douté et al.[27] report a broad chemical analysis of 79-mol% alkanes, 10-mol% cycloalkanes, and 11-mol% aromatics for the fuel utilized in their experimental investigation of kerosene flames. Furthermore, the chemical structures of *n*-decane and kerosene flames have been observed experimentally to exhibit marked similarities.[27] The chemical composition of kerosene, thus, is modeled in the present work by a surrogate blend comprising 89-mol% *n*-decane and 11-mol% aromatic fuel. The aromatic component is represented computationally by 1) benzene, 2) toluene, 3) ethylbenzene, and 4) ethylbenzene/naphthalene to investigate differences between various aromatic surrogates.

The reaction paths for *n*-decane are unaffected by the presence of the aromatic component, as generally observed for the interactive chemistry of individual species in fuel blends.[6,16] For the ethylbenzene aromatic constituent, the primary consumption (70%) paths are through C–C and C–H bond scission reactions. Hydrogen atom abstraction and addition reactions are observed to be secondary. The destruction of ethylbenzene ultimately passes through the benzene submechanism, and the consumption paths for benzene and the phenyl radical are entirely in agreement with previous observations in premixed systems.[1,6,16] Benzene growth through the recombination of C_2, C_3, and C_4 molecules accounts for only 5% of the total.

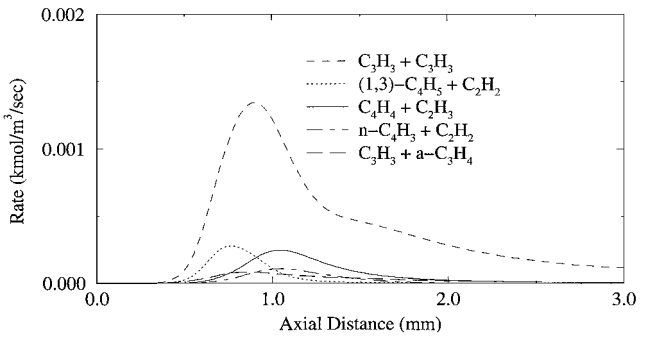

Fig. 10 Benzene formation channels in rich, atmospheric-pressure *n*-decane/O_2/N_2 laminar premixed flames.

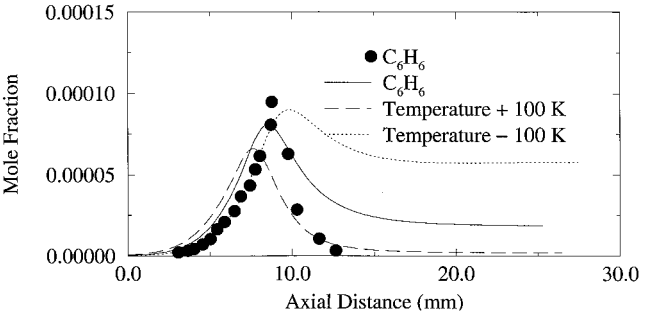

Fig. 12 Benzene concentrations in a rich, 0.06-bar *n*-decane laminar premixed flame; symbols indicate experimental data,[28] and lines indicate computations.

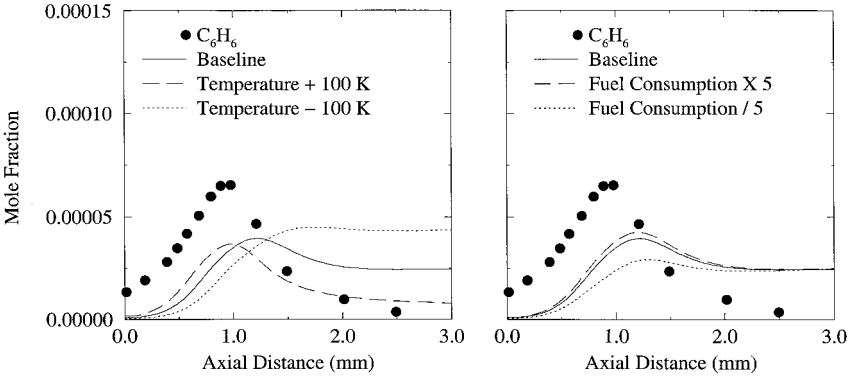

Fig. 11 Sensitivities of benzene concentrations to uncertainties in the temperature profile and the fuel consumption rates in rich, atmospheric-pressure *n*-decane/O_2/N_2 laminar premixed flames; symbols indicate experimental data,[27] and lines indicate computations.

Comparison with Experiments

The kerosene kinetic model has been evaluated at the experimental conditions of Douté et al.,[27] who measured the structure of a rich ($\phi = 1.7$), atmospheric-pressure, 2.95% kerosene/28.65% O_2/68.4% N_2 burner-stabilized laminar premixed flame. Temperature profiles and species concentration measurements were obtained using procedures as summarized earlier. Douté et al.[27] reported that the peak temperature measured for the kerosene flame was about 50°C higher than that observed for the *n*-decane flame. This is not surprising in view of the aromatic components of the kerosene flame.

Major species profiles for the atmospheric pressure *n*-decane and kerosene flames are nearly identical,[27] and comparisons between experimental and computed profiles are generally good. For example, CO and CO_2 concentrations are very well predicted (Fig. 13). The spatial profiles and lower peak concentrations of ethylene observed in the kerosene flame (Fig. 14) are captured remarkably well. The predicted concentration profiles for major species and ethylene are observed to be independent of the choice of aromatic component.

The fate of the aromatic constituents is of particular interest in the context of soot growth and pollutant emissions. Benzene concentrations measured in kerosene flames exceed those in *n*-decane flames by about an order of magnitude.[27] Comparison between experimental and computational benzene concentration profiles in the kerosene flame of Douté et al.[27] are shown in Fig. 15. Benzene is obviously a poor choice for the aromatic component of kerosene in the primary reaction zone. The order of magnitude increase in benzene concentrations, as well as the characteristic concentration profile, is reproduced well by the toluene, ethylbenzene, and ethylbenzene/naphthalene surrogates. The benzene concentration profile is again observed to be very sensitive to the uncertainties in the experimental temperature profile (Fig. 15).

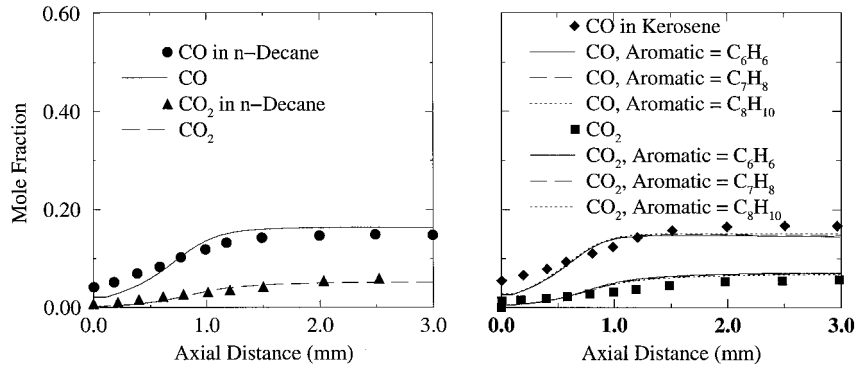

Fig. 13 CO and CO_2 concentrations in rich, atmospheric-pressure *n*-decane/O_2/N_2 and kerosene/O_2/N_2 laminar premixed flames; symbols indicate experimental data,[27] and lines indicate computations.

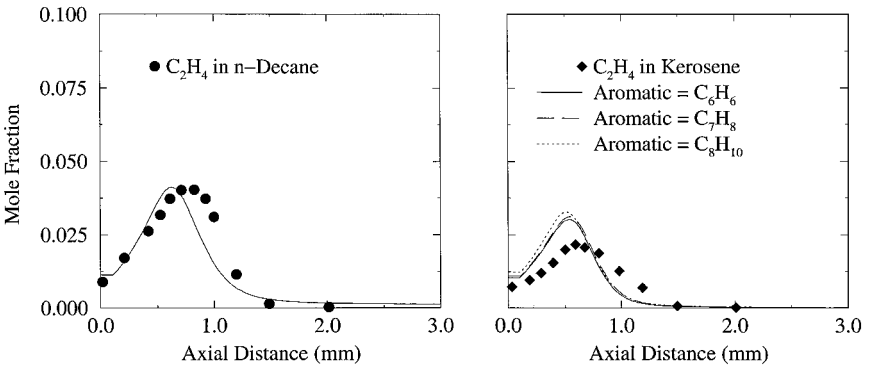

Fig. 14 C_2H_4 concentrations in rich, atmospheric-pressure *n*-decane/O_2/N_2 and kerosene/O_2/N_2 laminar premixed flames; symbols indicate experimental data,[27] and lines indicate computations.

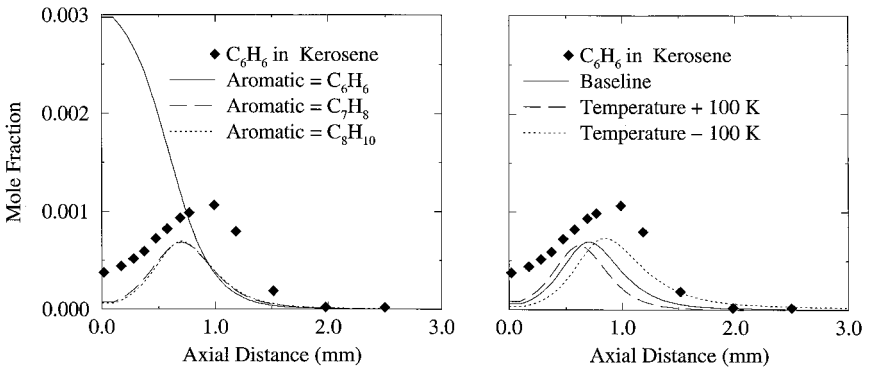

Fig. 15 Benzene concentrations in rich, atmospheric-pressure kerosene/O_2/N_2 laminar premixed flames; symbols indicate experimental data,[27] and lines indicate computations.

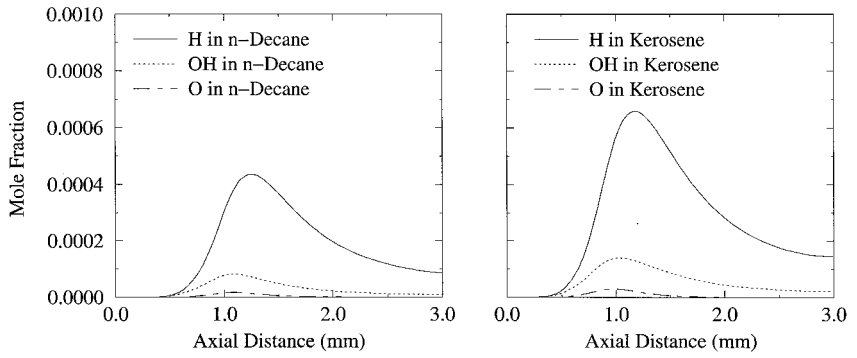

Fig. 16 Computed H, O, and OH concentrations in rich, atmospheric-pressure *n*-decane/O_2/N_2 and kerosene/O_2/N_2 laminar premixed flames.

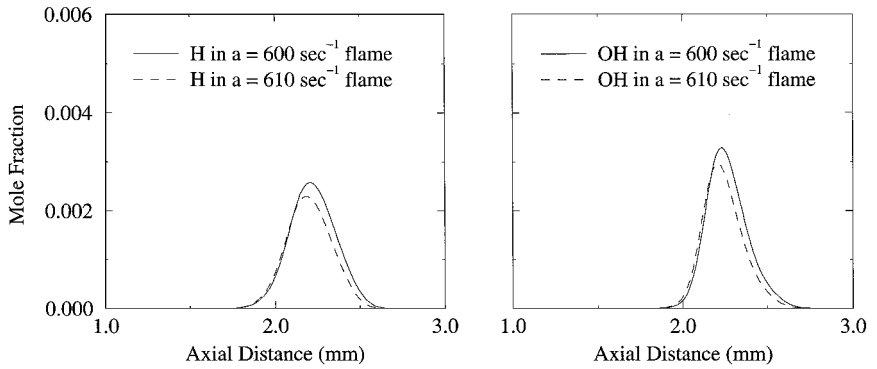

Fig. 17 Computed H and OH concentrations in stable and near extinction atmospheric-pressure *n*-heptane/air laminar diffusion flames; *a* denotes rate of strain.

Capabilities and Limitations of Kinetic Models for Aviation Fuels

The ability to accurately predict the composition of the exhaust of jet engines and the design of stable high-speed propulsion systems are the driving forces behind this effort. However, detailed reaction mechanisms comprising around 200 species and 1100 elementary reactions are presently too complex for direct application to multidimensional fluid dynamics problems. Simplified reaction mechanisms must be developed. However, simplified mechanisms are only as reliable as the detailed mechanism on which they are based.

The present detailed kinetic mechanism[16] appears capable of modeling the growth and destruction chemistry of benzene in kerosene flames and the growth chemistry of benzene in *n*-decane flames. Underpredictions of the benzene decay in the postflame zone of the present *n*-decane flames are shown to a large extent to be caused by uncertainties in the experimental temperature profile. The growth and destruction chemistry of benzene in flames of fuels comprising aromatic constituents are well reproduced. Moreover, the growth and destruction of MSA species in a variety of fuels are generally well predicted.[16] Thus, the present detailed mechanism appears a sound fundamental model on which to base simplified tools for predicting soot growth and pollutant formation in gas-turbine engines. Nevertheless, further refinement of the detailed mechanism may well be necessary as additional experimental data, including PAH measurements and free radical profiles for practical aviation fuels, becomes available. Moreover, the mechanism focus on high-temperature chemistry, the mechanism should also be further refined and evaluated to address practical aviation fuels ignition issues. Such an undertaking is hindered by lack of experimental data.

The detailed kinetic mechanism also appears capable of predicting the basic structure of kerosene and *n*-decane flames. Predictions of radicals in the 0.06-bar *n*-decane flame of Delfau et al.[28] were adequate. However, experimental measurements for direct comparison to predicted H and O atoms and OH radical concentrations in kerosene flames are not available, and more detailed predictive capabilities are not implied by the present work. Consequently, a discussion of similarities and differences observed in the computed radical pools of *n*-decane and kerosene flames is interesting. The computed profiles for H and O atoms and the OH radical in *n*-decane and kerosene flames at the experimental conditions of Douté et al.[27] are shown in Fig. 16. The characteristic profiles of the key radicals are very similar, but the higher temperatures observed in the kerosene flame result in a higher radical pool. The relative importance of the differences noted is best viewed in terms of flame extinction considerations. The H atom and OH radical concentrations in stable and near extinction atmospheric *n*-heptane/air laminar diffusion flames[3] are shown in Fig. 17. Dissimilarities are less pronounced than those resulting from the temperature differences in *n*-decane and kerosene flames. Therefore, an understanding of the uncertainty bands inevitably associated with any kinetic mechanism is a prerequisite when using simplified kinetic models to predict flame stability in high-speed propulsion systems. Further evaluation of the detailed mechanism against measured key radicals in kerosene flames is necessary, as such data become available.

Conclusions

A detailed chemical–kinetic reaction mechanism has been extended to consider the gas- phase chemistry of model practical aviation fuels. The structures of *n*-decane and kerosene laminar premixed flames have been studied in detail, and the most remarkable difference observed was an order of magnitude increase in benzene concentrations in the kerosene flame. It has been shown that the structure of premixed kerosene flames can be predicted accurately using *n*-decane/alkyl-substituted aromatic surrogate blends. Nevertheless, refinement of the surrogate model to account for other kerosene constituents will be necessary to predict additional minor species.

Collectively, comparisons between experiments and computations for 25 major, stable intermediate and radical species are reported. Major species are generally predicted within 15%, with the worst disagreement being about 50% for one case: hydrogen

concentrations in the postflame of the atmospheric pressure kerosene flame of Douté et al.[27] Predictions for intermediate and radical species are remarkably accurate and within established experimental and mechanistic uncertainties. Agreement between computations and experiments for the rate of benzene growth in *n*-decane flames is reasonable given experimental uncertainties in the temperature profiles. Good agreement between computations and experiments was obtained for benzene concentrations in a kerosene flame, where benzene formation occurs primarily through the decomposition of the aromatic constituents. It is proposed that the present detailed kinetic mechanism for aviation fuels is a sound basis for future simplifications aimed to address practical problems such as soot growth, pollutant formation, and flame stability in practical combustors.

References

[1]Lindstedt, R. P., and Skevis, G., "Detailed Kinetic Modeling of Premixed Benzene Flames," *Combustion and Flame*, Vol. 99, Nos. 3, 4, 1994, p. 551.

[2]Leung, K. M., and Lindstedt, R. P., "Detailed Kinetic Modeling of C_1–C_3 Alkane Diffusion Flames Flames," *Combustion and Flame,* Vol. 102, Nos. 1, 2, 1995, p. 129.

[3]Lindstedt, R. P., and Maurice, L. Q., "Detailed Kinetic Modelling of *n*-Heptane Combustion," *Combustion Science Technology*, Vol. 107, Nos. 4, 6, 1995, p. 317.

[4]Leung, K. M., "Kinetic Modeling of Hydrocarbon Flames Using Detailed and Systematically Reduced Chemistry," Ph.D. Thesis, Univ. of London, Imperical College, Mechanical Engineering Dept., England, UK, Oct. 1995.

[5]Lindstedt, R. P., and Skevis, G., "A Study of Acetylene Chemistry in Flames," *Combustion Science Technology*, Vol. 125, Nos. 1, 6, 1997, p. 73.

[6]Lindstedt, R. P., and Maurice, L. Q., "Detailed Kinetic Modeling of Toluene Combustion," *Combustion Science Technology*, Vol. 120, Nos. 1, 6, 1996, p. 119.

[7]Lipinski, J., Armstrong, J., Johnson, R., White, C., and Kretzinger, K., "Design, Fabrication and Testing of a Boilerplate Endothermic Methylcyclohexane Fuel Heat Exchanger Reactor System," AFWRDC-TR-89-204, Dayton, OH, June 1989.

[8]Sobel, D. R., and Spadaccini, L. J., "Hydrocarbon Fuel Cooling Techniques for Advanced Propulsion," American Society of Mechanical Engineers, Turbo EXPO 95, ASME Paper 95-GT-226, Houston, TX, June 1995.

[9]Edwards, T., "Recent Research Results in Advanced Fuels," *American Chemical Society Petroleum Chemistry Division Preprints*, Vol. 41, No. 2, 1996, p. 481.

[10]Salooja, K. C., "Studies of Combustion Processes Leading to Ignition of Isomeric Hexanes," *Combustion and Flame,* Vol. 6, No. 4, 1962, p. 275.

[11]Richards, G. A., and Lefebvre, A. H., "Turbulent Flame Speeds of Hydrocarbon Fuel Droplets in Air," *Combustion and Flame*, Vol. 78, 1989, p. 299.

[12]Guéret, C., Cathonnet, M., Boettner, J. C., and Gaillard, F., "Experimental Study and Modeling of Kerosene Oxidation in a Jet-Stirred Flow Reactor," *Twenty-Third Symposium (International) on Combustion*, Combustion Inst., Pittsburgh, PA, 1990, p. 211.

[13]Dagaut, P., Reuillon, M., Boettner, J. C., and Cathonnet, M., "Kerosene Combustion at Pressures up to 40 Atm: Experimental Study and Detailed Chemical Kinetic Modeling," *Twenty-Fifth Symposium (International) on Combustion*, Combustion Inst. Pittsburgh, PA, 1994, p. 919.

[14]Ranzi, E., Sogaro, A., Gaffuri, P., Pennati, G., Westbrook, C. K., and Pitz, W. J., "A New Comprehensive Reaction Mechanism for Hydrocarbon Fuels," *Combustion and Flame,* Vol. 99, 1994, p. 201.

[15]Vovelle, C., Delfau, J. L., and Reuillion, M., "Formation of Aromatic Hydrocarbons in Decane and Kerosene Flames at Reduced Pressures," *Soot Formation in Combustion: Mechanisms and Models*, edited by H. Bockhorn, Springer–Verlag, Berlin, 1994, pp. 50–65.

[16]Maurice, L. Q., "Detailed Chemical Kinetic Models for Aviation Fuels," Ph.D. Thesis, Univ. of London, Imperical College, Mechanical Engineering Dept., London, England, UK, Dec. 1996.

[17]Warnatz, J., "Chemistry of High Temperature Combustion of Alkanes up to Octane," *Twentieth Symposium (International) on Combustion,* Combustion Inst., Pittsburgh, PA, 1984, p. 845.

[18]Chakir, A., Belliman, M., Boettner, J. C., and Cathonnet, M., "Kinetic Study of *n*-Heptane Oxidation," *International Journal of Chemical Kinetics*, Vol. 24, No. 4, 1992, p. 385.

[19]Gonzales, M. G., Lew, L., and Cunningham, R. E., "Determinacion de la Cinetica de Descomposicion Termica de Alcoholes e Hydrocarburos Mediante un Reactor Pulso," Laboratorio Ensayo Material Investigacion Tecnologica, Madrid, 1971, p. 103.

[20]Rumyantsev, A. N., Shevel'kova, L. V., Sokolova, V. M., and Nametkin, N. S., "Dependence of the Decomposition Rate Constant of Higher *n*-Paraffin Hydrocarbons on Their Molecular Weight," *Neftekhim,* Vol. 20, March 1980, p. 212.

[21]Miller, J. A., Kee, R. J. and Westbrook, C. K., "Chemical Kinetics and Combustion Modeling," *Annual Review of Physics and Chemistry,* Vol. 41, June 1990, p. 345.

[22]Warnatz, J., "The Structure of Laminar Alkane, Alkene, and Acetylene Flames," *Eighteenth Symposium (International) on Combustion,* Combustion Inst., Pittsburgh, PA, 1980, p. 369.

[23]Foelsche, R. O., Keen, J. M., and Solomon, W. C., "A Non-Equilibrium Computational Method for Predicting Fuel Rich Gas Generator Performance and Exhaust Properties—Volume II: Reaction Kinetics and Computational Results," Univ. of Illinois Rept. AAE9307, UIL93-0507, Urbana–Champaign, IL, March 1993.

[24]Westbrook, C. K., Pitz, W. J., and Warnatz, J., "A Detailed Chemical Kinetic Reaction Mechanism for the Oxidation of *iso*-Octane and *n*-Heptane over an Extended Temperature Range," *Twenty-Second Symposium (International) on Combustion,* Combustion Inst., Pittsburgh, PA, 1988, p. 893.

[25]Jones, W. P., and Lindstedt, R. P., "Global Reaction Schemes for Hydrocarbon Combustion," *Combustion and Flame,* Vol. 73, Nos. 1, 3, 1988, p. 233.

[26]Jones, W. P., and Lindstedt, R. P., "The Calculation of the Structure of Laminar Counterflow Diffusion Flames Using a Global Reaction Mechanism," *Combustion Science Technology*, Vol. 61, Nos. 1, 6, 1988, p. 31.

[27]Douté, C., Delfau, J. L., Akrich, R., and Vovelle, C., "Chemical Structure of Atmospheric Pressure Premixed *n*-Decane and Kerosene Flames," *Combustion Science Technology*, Vol. 106, Nos. 4, 6, 1995, p. 327.

[28]Delfau, J. L., Bouhria, M., Reuillon, M., Sanogo, O., Akrich, R., and Vovelle, C., "Experimental and Computational Investigation of the Structure of a Sooting Decane-O_2-Ar Flame," *Twenty Third Symposium (International) on Combustion*, Combustion Inst., Pittsburgh, PA, 1990, p. 1567.

[29]Skevis, G., "Soot Precursor Chemistry in Laminar Premixed Flames," Ph.D. Thesis, Imperical College, Mechanical Engineering Dept., Univ. of London, London, England, UK, Dec. 1996.